Synchronverter-Enabled DC Power Sharing Approach for LVDC Microgrids

Peyghami, Saeed; Davari, Pooya; Mokhtari, Hossein; Loh, Poh Chiang; Blaabjerg, Frede

Published in:
I E E E Transactions on Power Electronics

DOI (link to publication from Publisher):
10.1109/TPEL.2016.2632441

Publication date:
2017

Document Version
Accepted author manuscript, peer reviewed version

Synchronverter-enabled DC Power Sharing Approach for LVDC Microgrids

Saeed Peyghami[1], *Student Member, IEEE,* Pooya Davari[2], *Member, IEEE,*
Hossein Mokhtari[1], *Senior Member, IEEE,* and Frede Blaabjerg[2], *Fellow, IEEE*

***Abstract*— In a classical ac Micro-Grid (MG), a common frequency exists for coordinating active power sharing among droop-controlled sources. Like the frequency droop method, a voltage based droop approach has been employed to control the converters in dc MGs. However, voltage variation due to the droop gains and line resistances causes poor power sharing and voltage regulation in dc MG, which in most cases are solved by a secondary controller using a communication network. To avoid such an infrastructure and its accompanied complications, this paper proposes a new droop scheme to control dc sources by introducing a small ac voltage superimposed onto the output dc voltage of converters. Therefore, dc sources can be coordinated together with the frequency of the ac voltage, without any communication network like Synchronous Generators (SGs) in conventional power systems. Small signal stability analysis as well as mathematical calculations are presented to demonstrate the analogy between the proposed strategy and frequency-based droop approach of the SGs. The effectiveness of the proposed control system is evaluated by simulations and verified by experiments.**

***Index Terms*— dc microgrid, droop method, power sharing, synchronverter.**

I. Introduction

DC MG is a reliable, efficient and low-cost technology to integrate the renewable resources and storages into distribution systems as well as to be used in remote applications [1]–[3]. To have a stable operation of different type of energy sources, a power management system is required to control and coordinate different power converter units. Meanwhile, without a proper power management strategy, overstressing of the converters at steady state may damage the units. Furthermore, a supervisory controller is required in order to regulate the dc voltages within an acceptable region [4]–[6].

Voltage droop methods have recently been used to control the converters at primary level [4], [5], [7]–[10]. However, these methods suffer from poor power sharing and voltage regulation due to the droop gains and line impedances. To improve the power sharing accuracy as well as voltage regulation, modified droop methods, reinforced by a communication network, are presented in dc [9], [11]–[14]. A distributed secondary average voltage and average current regulators are presented in [9] to improve the effectiveness of the primary droop controller. A cooperative decentralized droop method based on dynamic consensus protocol is also presented in [11] by utilizing the sparse communication network among converters. Furthermore, in [12], a decentralized secondary controller based on a pilot bus regulation function through low-bandwidth communication is introduced to compensate the voltage drops caused by primary droop controllers. However, in [9], [11], [12], a secondary control layer is employed to compensate the voltage drops raised by droop gains. Implementing secondary controller by a communication network to share the information of voltage and current of converters may affect the stability and reliability of the system. Moreover, a non-linear droop approach is presented in [15] to reduce the effect of droop controller on voltage drops as well as to improve the current sharing accuracy. However, the stability of the system is questionable due to the non-linear droop characteristics.

In [16], a load-sharing approach based on frequency encoding of output current of converters has been introduced, which requires no communication link. In another technique in [15], named as Power Talk, sources in the dc MG "talk" to each other by modulating their respective power levels without utilizing any external communication link. The approach is however prone to line, load, and other grid parameter changes, which in practice, are unpredictable. The frequency-based power sharing technique proposed in [17] and [18], and later reapplied to dc microgrids in [19] may therefore be more appealing, since it is based on the same conventional droop principle, while yet ensuring very low affection towards variations. However, this approach is not applicable for low voltage dc power systems.

Aforementioned issues – inaccurate load sharing, large voltage drop, and utilizing communication system – arise due to the lack of a global control variables in dc MGs unlike in ac MGs. In traditional ac power systems, SGs are coordinated together with a frequency droop control of the governor system [20]. In ac MGs, power electronic-based units, also called synchronverter or virtual synchronous generator, are coordinated together with a frequency droop controller as well [10], [21]–[23]. However, in dc microgrids, dc voltage is the only control parameter which is not a unique variable within the microgrid.

In this paper, the concept of synchronverter is utilized to control the converters in dc MGs. A superimposed frequency injected by the converters is used to coordinate them together in order to improve the power sharing accuracy and voltage regulation, and consequently the reliability. Conventional voltage droop controller and the proposed control approach are explained in Section II, and the small signal modeling as well as the stability analysis are given in Section III. In

[1] Saeed Peyghami and Hossein Mokhtari are with the Department of Electrical Engineering, Sharif University of Technology, Iran (e-mail: saeed_peyghami@ee.sharif.edu, mokhtari@sharif.edu).

[2] Pooya Davari and Frede Blaabjerg are with the Department of Energy Technology, Aalborg University, Denmark (e-mail: pda@et.aau.dk, fbl@et.aau.dk).

Section IV, mathematical analysis shows the converters controlled by the proposed control approach mimics an SG. Simulations and experimental results are respectively given in Section V and Section VI in order to evaluate the viability and applicability of the proposed strategy. Finally, Section VII summarizes the achievements.

II. Power Sharing Control Approach

The conventional voltage droop controller are employed for power sharing among converters in a dc microgrids. However it suffers from poorer power sharing and voltage regulation due to the droop gains and line impedances. The conventional voltage droop approach and the proposed frequency droop approach are explained in the following.

A. Conventional Voltage Droop Approach

Droop controller as a primary load sharing method, locally determines the reference current of each converters by employing the corresponding output current and/or voltage. As shown in Fig. 1(a), the primary droop control of the k^{th} converter adapts the set point of the inner voltage regulator utilizing a virtual resistor R_{dk} multiplied by the output current (I_{ok}). Hence, according to Fig. 1(a), the output current and voltage of converters employing the droop controller can be found by solving (1) and (2) as:

$$\begin{cases} V_{o1} = V_{PCC} + R_1 I_{o1} \\ V_{o2} = V_{PCC} + R_2 I_{o2} \end{cases}, \tag{1}$$

$$\begin{cases} V_{o1} = V^* - R_{d1} I_{o1} \\ V_{o2} = V^* - R_{d2} I_{o2} \end{cases}, \tag{2}$$

where V^* is the nominal voltage of the microgrid. This can be graphically determined as shown in Fig. 1(b) for small and large droop gains $R_{d1} < R_{d2}$. As it can be seen from Fig. 1(b), the mismatch between the output currents in the case of larger droop gain R_{d2} is smaller than the smaller droop gain R_{d1} (i.e., $\Delta I_2 < \Delta I_1$). However, increasing the droop gain causes a larger voltage drop. As it can be seen from Fig. 1(b), the voltage drop of the larger droop gain is higher than the voltage drop of the smaller one (i.e., $\Delta V_1 < \Delta V_2$). Therefore, improving the current sharing accuracy deteriorates the voltage regulation [7], [11]. In order to achieve the accurate load sharing, large droop gains can be used, and hence to restore the voltage drop of the large droop gains, a secondary control layer is employed as shown in Fig. 1(a), which is explained in the following.

The output of the central controller, as a restoration term δ_v, is sent to all of the units to shift up their droop characteristics as shown in Fig. 1(c). To implement the central voltage regulator, a communication network is required between the central controller and converters, which affects the reliability and stability.

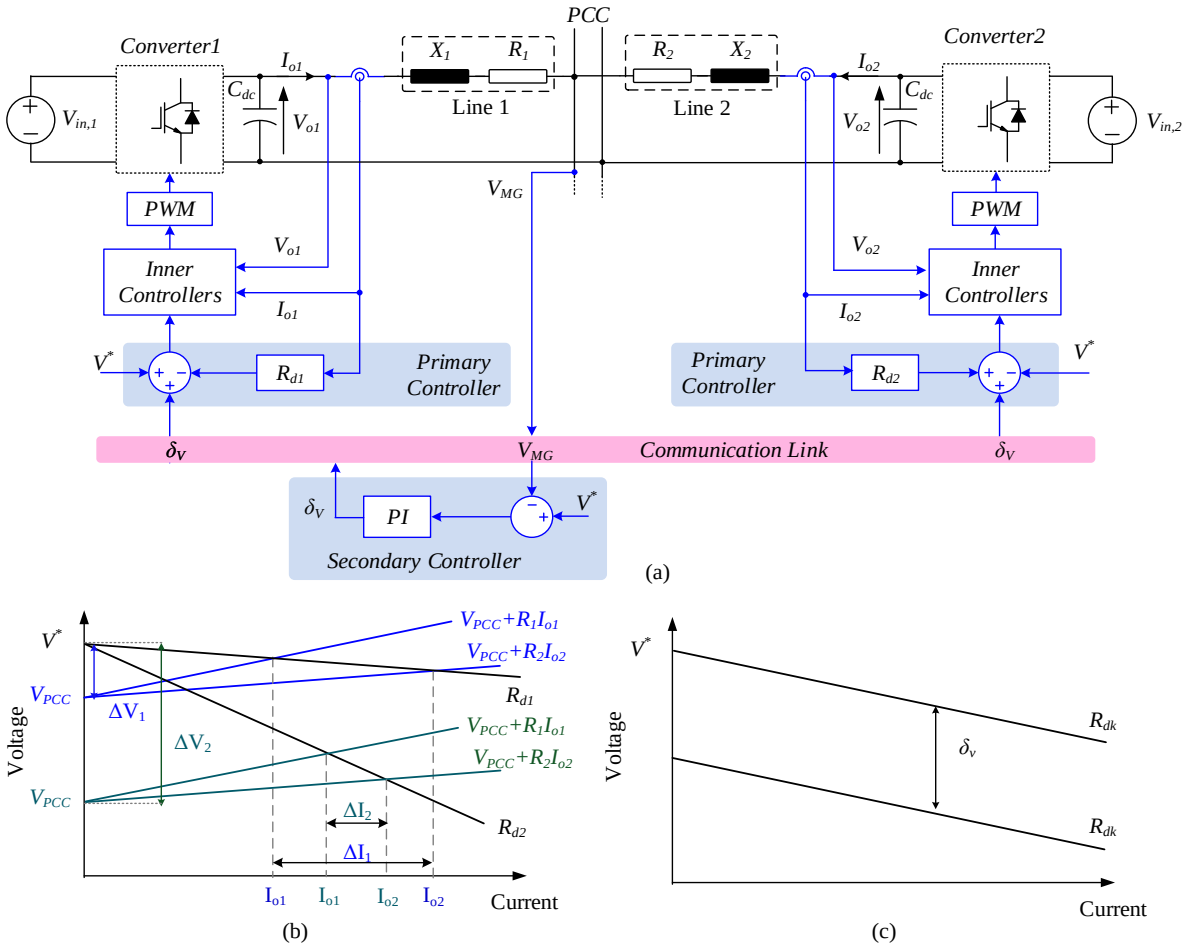

Fig. 1. Concept of conventional droop controller in a dc microgrid, (a) Schematic and control block diagram of a primary and secondary controller for a simplified dc microgrid, (b) effect of different droop gains in primary level, (b) effect of secondary controller.

To improve the overall reliability and stability, some decentralized approaches are represented [24], [25]. In these approaches, sparse communication among the neighboring converters is employed, and a dynamic consensus protocol based control algorithm guarantees the voltage regulation in the microgrid. Either centralized or decentralized secondary layer require communicating the current and voltage information among the converters. To avoid such an infrastructure and its accompanied complications as well as to improve the reliability and stability of the system, in the next section, a proposed load sharing approach without a communication network is presented.

B. Proposed Frequency Droop Approach

A typical dc MG with distributed loads is shown in Fig. 2 (a). The dc sources can be a dispatchable unit such as fuel cell module or a hybrid battery/non-dispatchable unit such as photovoltaic array, which can control the dc link voltage as a voltage source converter. The proposed control approach for the k^{th} unit is shown in Fig. 2(b). Each converter modulates a small ac voltage superimposed onto the dc voltage, where the frequency of the ac voltage is proportional to the output dc current of the converter. The rated frequency should be selected smaller than the bandwidth of the inner voltage controller to be regulated by a Proportional- Integrator (PI) based voltage regulator. Therefore, the inner voltage ($G_v(s)$) and current ($G_i(s)$) controllers in Fig. 2(c) can modulate the reference voltage including dc voltage and superimposed ac voltage. From the ac voltage point of view, the converters are working like an SG, and hence they can be coordinated together with the common frequency. From the power system dynamics and control theory, for analyzing the dynamic behavior of an SG in an ac power system, it can be modeled as two SG; one being the specified SG and another modeling the entire power system. Moreover, the two SG can be simplified as a single-machine-infinite-bus, where the infinite bus is considered as a stiff ac source [20]. Therefore, since the proposed approach is based on the SG principles, without losing the generality, a simplified dc MG, with two converters connected to a load at a Point of Common Coupling (PCC) is considered, and the block diagram of the system with the corresponding signals are shown in Fig. 3. According to Fig. 3, if the output dc voltage of the converters (V_{o1}, V_{o2}) is settled at a reference value (V_o^*), the output dc current of them (I_{o1}, I_{o2}) will be inversely proportional to the corresponding line resistances (i.e., $I_{o1}/I_{o2} = R_2/R_1$), where R_1 and R_2 denote the line resistance of the first and second converter, respectively. Adjusting the output dc voltage of the converters is the only option to control the corresponding output currents at a desired value, for example proportional to their rated current, which requires the coordination of converters. To make a coordination between converters, a small ac voltage, i.e., $\tilde{v}_k = A.sin(2\pi f_k t)$, is superimposed onto the dc voltage reference and modulated by each converter. The amplitude of the superimposed voltage (denoted as A) is considered to be a small constant value to have a small ripple factor, however it should be detectable by the measurements. Furthermore, the corresponding frequency should be proportional to the output current of the converter, and it can be defined as:

$$f_k = f^* - d_{fk} i_{ok} \tag{3}$$

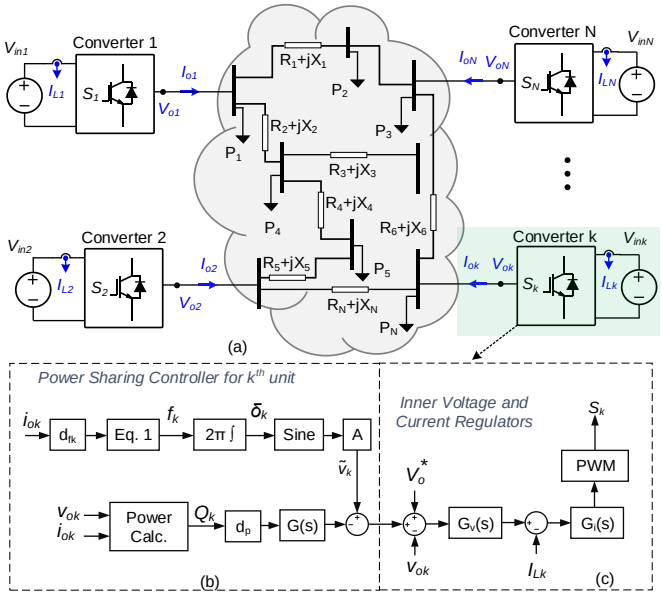

Fig. 2. Block diagram of (a) a typical dc MG with distributed loads, (b) proposed control structure for k^{th} converter, (c) inner voltage and current control loops – G_v(s) and G_i(s) are PI-based inner voltage and current controllers (PI: Proportional-Integrator), $\tilde{v}_k = A.sin(2\pi f_k t)$ is the superimposed ac voltage, where A and f_k is the corresponding amplitude and frequency.

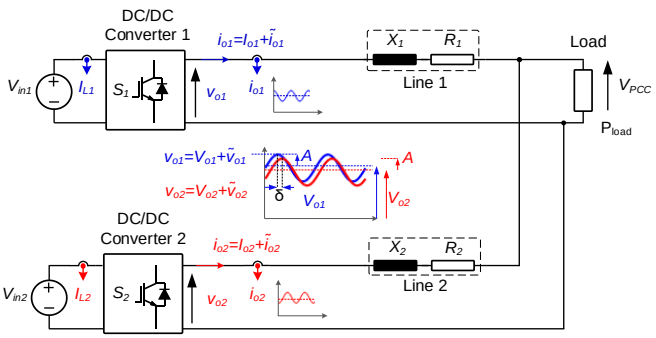

Fig. 3. Conceptual illustration of the proposed strategy showing the injected ac voltages and corresponding currents in a simplified dc MG based on two dc-dc converters.

where f^* (50 *Hz*) is the nominal frequency, i_{ok} being the output current, and d_{fk} is the frequency droop gain of k^{th} converter determined by

$$d_{fk} = \frac{f_{\max} - f_{\min}}{I_{n,k}}; \quad k = 1,2 \tag{4}$$

with f_{max}/f_{min} being the maximum/minimum frequency for tuning the droop gain and $I_{n,k}$ is the nominal current of k^{th} converter. At steady state condition, the frequency of the units has the same value, and hence, the output current of the units has to be shared proportional to their rated current as shown in (5), where $<x>$ denotes the average of x and ξ is the ratio of the rated current of the converters.

$$\frac{<i_{o1}>}{<i_{o2}>} = \frac{I_{o1}}{I_{o2}} = \frac{I_{n,1}}{I_{n,2}} = \frac{d_{f2}}{d_{f1}} = \xi \tag{5}$$

Frequency droop can be used to coordinate the converters by a common injected frequency. Therefore, the dc currents need to be regulated by the frequency to control the power sharing. However, the dc currents are determined by the dc voltages as:

$$I_{o1}=\frac{V_{o1}-V_{PCC}}{R_1};\ I_{o2}=\frac{V_{o2}-V_{PCC}}{R_2} \tag{6}$$

with R_1 and R_2 being the line resistances. Therefore, the dc voltages should be adjusted by an ac injected variable related to the frequency. According to Fig. 3 and (5), the phase angle of each unit (δ_1, δ_2) can be found as:

$$\delta_1=\frac{2\pi}{s}\left(f^*-d_{f1}I_{o1}\right),\quad \delta_2=\frac{2\pi}{s}\left(f^*-d_{f2}I_{o2}\right) \tag{7}$$

where, s is the Laplace operator. The relative phase (δ) between the converters is thus equal to:

$$\delta=\delta_1-\delta_2=\frac{2\pi}{s}\left(d_{f2}I_{o2}-d_{f1}I_{o1}\right) \tag{8}$$

If the output currents are not proportional to the rated currents, the phase angle will not be zero. Hence, this phase difference causes a small ac power flow. As the load impedance is higher than the line impedances, the small ac power will only flow between the converters. According to the ac power flow theory, ac power is proportional to the ac currents ($\tilde{i}_1$, $\tilde{i}_2$). Furthermore, the ac currents are proportional to the line impedances. Thereby, the ac power contains the information of the line impedances. On the other hand, in LV systems with low *X/R* ratio, the reactive power can properly be controlled by the frequency [26]. Therefore, employing the injected reactive power (Q) of the converters to adjust the dc voltage reference (V_o^*) causes a proper current sharing. Applying the proposed control algorithm, the output dc voltage of the converters can be written as:

$$V_{o1}=V_o^*-d_pQ_1G(s),\ \ V_{o2}=V_o^*-d_pQ_2G(s) \tag{9}$$

in which d_p is the coupling gain between dc voltage and reactive power, and $G(s) = \omega_c/(s+\omega_c)$ is a low pass filter to eliminate the high frequency component of the calculated reactive power. Therefore, the frequency droop can be used to coordinate the converters, and the small ac power can be employed to adjust the dc voltage and consequently the dc currents. Each converter can be controlled by the local measured values, and hence, like SGs, there is no need for any communication network. Furthermore, the injected ac voltage by the converters has to be synchronized with the ac component of the grid voltage at the startup time. The phase of the connection bus voltage can be extracted using a Phase Locked Loop (PLL) block. On the other hand, in ac systems, synchronization methods are employed to make the converter voltage close to the grid voltage in order to limit the inrush current at the starting time, which may damage the converter switches for the large amount of currents. However, the injected ac voltage and consequently the ac currents are very small in the proposed approach and hence the converters can be connected together without utilizing a PLL. Hence, they can be synchronized based on the droop controller functionality like the grid supporting voltage source converters in ac microgrids [27].

III. Small Signal Modeling and Stability

Based on the ac power flow analysis, and considering a low *X/R* ratio for line impedances, the reactive power generated by both converters, Q_1 and Q_2 can be calculated as:

$$Q_1=-\frac{A^2/2}{R_1+R_2}\sin\delta,\quad Q_2=\frac{A^2/2}{R_1+R_2}\sin\delta \tag{10}$$

where A is the amplitude of the injected voltage. The linear form of (8), (9), and (10) at $\delta = \delta_0$ can be written as (11), (12), and (13) respectively.

$$\Delta\delta=\frac{2\pi}{s}\left(d_{f2}\Delta I_{o2}-d_{f1}\Delta I_{o1}\right) \tag{11}$$

$$\Delta Q_1=-k_\delta\Delta\delta,\ \ \Delta Q_2=+k_\delta\Delta\delta;\ \ k_\delta=\frac{A^2}{2\left(r_1+r_2\right)}\cos\delta_0 \tag{12}$$

$$\Delta V_{o1}=-d_p\Delta Q_1G(s),\quad \Delta V_{o2}=-d_p\Delta Q_2G(s) \tag{13}$$

Considering load power and voltage equal to P_{load} and V_{PCC}, then:

$$P_{load}=V_{PCC}(I_{o1}+I_{o2})\,. \tag{14}$$

The linear form of (6) and (14) can be written as:

$$\begin{cases}\Delta V_{o1}=\Delta V_{PCC}+R_1\Delta I_{o1}\\ \Delta V_{o2}=\Delta V_{PCC}+R_2\Delta I_{o2}\end{cases} \tag{15}$$

$$\Delta V_{PCC}=-R_0\Delta I_{o1}-R_0\Delta I_{o2}+\frac{\Delta P_{load}}{I_{10}+I_{20}};\quad R_0=\frac{V_{PCC0}}{I_{10}+I_{20}} \tag{16}$$

where I_{10} and I_{20} are the dc current of each converter at $V_{PCC} = V_{PCC0}$. Combining equations (11)-(16), and considering $\Delta\delta$ as a state variable and ΔP_{load} as a disturbance, the state space representation can be found as:

$$\frac{d^2\Delta\delta}{dt^2}+\omega_c\frac{d\Delta\delta}{dt}+\frac{\beta}{\alpha}\Delta\delta=\frac{\gamma\omega_c}{\alpha}\Delta P_{load}+\frac{\gamma}{\alpha}\frac{d\Delta P_{load}}{dt} \tag{17}$$

and α, β, γ can be defined as:

$$\alpha=R_1R_2-\left(R_1+R_2\right)R_0 \tag{18}$$

$$\beta=2\pi\omega_ck_\delta d_{f1}d_p\left(R_1\xi+R_2-2R_0\left(\xi+1\right)\right) \tag{19}$$

$$\gamma=\frac{2\pi d_{f1}\left(R_2-\xi R_1\right)}{I_{10}+I_{20}} \tag{20}$$

Equation (17) shows the dominant poles of the closed loop system. According to the control theory, a closed loop system is dynamically stable if $d_{f1}d_p > 0$. In order to show the dynamic response of the system with the parameters given in TABLE I, the closed-loop dominant pole places in terms of d_p and d_{f1} are depicted in Fig. 4(a) and (b) respectively. Consequently, the control parameters are designed to locate the closed loop poles at the places shown in Fig. 4(c) to have a damping ratio higher than 0.7, which requires d_{f1} = 0.15, d_p = 15 for ξ = 1, 2. Furthermore, as it can be seen in Fig. 4(d), the closed loop system is not significantly affected by the load variation.

According to (12) and (19), the superimposed voltage (A) can also affect the closed loop poles of the system. The ac voltage should be selected small enough to have an acceptable ripple factor as well as large enough to be measurable. Therefore, for the selected value of the ac voltage, a desired system damping ratio can be achieved by a suitable value of the voltage-power coupling gain (d_p) based on (12) and (19). For instance, selecting the voltage-power coupling gain of d_p = 15 and ac voltage of A = 2.5 *V*, the desired damping ratio of 0.7 can be achieved for the system described in Table I.

TABLE I
PARAMETERS OF THE POWER SYSTEM CONTROLLERS

Parameter	Symbol	Value
DC link voltage	V^*	400 V
Injected voltage	A	2.5 V (0.625 %)
Nominal injected frequency	f^*	50 Hz
Load	P_{load}	2500 W
Line Resistance	R_1, R_2	2.5, 1.5 Ω
Converter rating ratio	ξ	1, 2
Voltage – power coupling gain	d_p	15
Frequency droop gain	d_{f1}, d_{f2}	0.15, $\xi \times 0.15$
Cut-off frequency	ω_c	35 rad/s
DC inductor of Converters	L_{dc}	2 mH
DC capacitor of Converters	C_{dc}	500 μF

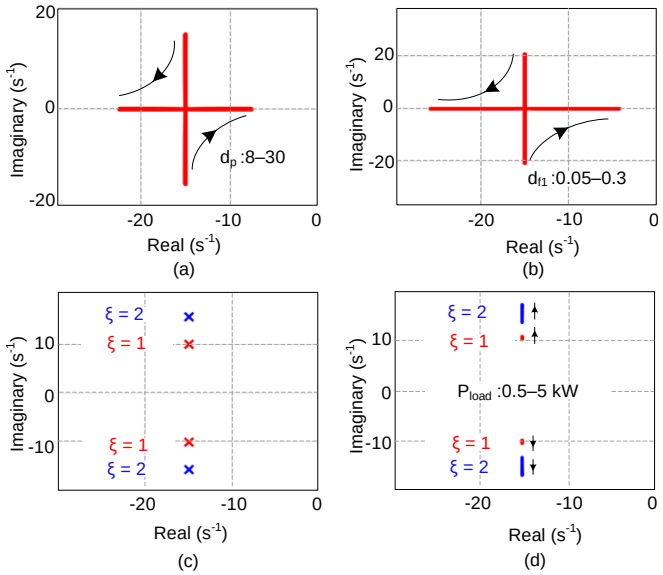

Fig. 4. Closed loop dominant pole locations of the control system (a) effect of d_p, d_{f1} = 0.15, ξ = 1, P_{load} = 2.5 kW, (b) effect of d_{f1}, d_p = 15, ξ = 1, P_{load} = 2.5 kW, (c) designed closed loop pole places, and (d) effect of P_{load} on designed pole places, d_p = 15, d_{f1} = 0.15, ξ = 1, 2.

IV. RELATIONSHIP WITH SYNCHRONOUS GENERATOR

In this section, mathematical analysis is presented in order to make a relationship between the proposed droop controlled dc MG and an SG. In the conventional power systems, load-frequency controller is utilized to balance the load and generation, where increasing the load decreases the rotational speed of the generator. Therefore, the governor system detects the speed reduction and increases the mechanical power. In the case of single machine based power system, the governor regulates the speed and frequency at a nominal value. However, operating parallel SGs requires sharing the load among them, which is done by the frequency-droop controller. Therefore, the corresponding governor can determine the reference power dictated by the droop gain. In this paper, the conventional load-frequency control concept is applied for dc MGs and the analogies between the conventional SGs and proposed dc synchronverters is analyzed in the following.

According to [20], the swing equation of an SG connected to an infinite bus can be defined as:

$$P_m - P_e = J\frac{d^2\delta}{dt^2} + D\frac{d\delta}{dt}, \tag{21}$$

where δ is the rotor angle, J is the rotor inertia, D is the damping factor, and P_m/P_e is the per-unit mechanical/electrical power. The small signal representation of (21) can be written as:

$$\frac{d^2\Delta\delta}{dt^2} + \frac{D}{J}\frac{d\Delta\delta}{dt} = \frac{1}{J}(\Delta P_m - \Delta P_e). \tag{22}$$

Furthermore, the electrical power flowed between an SG and an infinite bus can be determined as:

$$P_e = \frac{E^2}{X}\sin\delta, \tag{23}$$

where E is the sending and receiving end voltages, X is the line reactance, and δ is the phase angle between the SG and infinite bus. The linear form of (23) can be obtained as:

$$\Delta P_e = \frac{E^2}{X}\cos\delta\cdot\Delta\delta, \tag{24}$$

and the synchronization torque (power) factor is defined as:

$$k_1 = \frac{E^2}{X}\cos\delta. \tag{25}$$

Therefore, the small signal model of the swing equation can be rewritten as:

$$\frac{d^2\Delta\delta}{dt^2} + \frac{D}{J}\frac{d\Delta\delta}{dt} + \frac{k_1}{J}\Delta\delta = \frac{1}{J}\Delta P_m. \tag{26}$$

The small signal model of the dc synchronverter is given in (17), where (17) is the counterpart of (26), and hence, the proposed droop method for two dc-dc converters mimics the behavior of an SG connected to an infinite bus. A list of analogies and differences between these two equations are given in the following.

1) The variable of ω_c in (17), corresponds completely to D/J in (26). Also, β/α in (17), is the counterpart of k_1/J in (26). Moreover, according to (19) β is proportional to k_δ which is defined in (12), hence the synchronization torque (power) factor k_δ in (12) is analogous with k_1 in (25). Therefore, the damping, inertia and the synchronization torque factor in the swing equation of the SG are emulated in the dc MG by the proposed frequency droop characteristics.
2) The disturbance term $(\gamma\omega_c/\alpha)\Delta P_{load}$ in (17) corresponds to the term $(1/J)\Delta P_m$ in (26). ΔP_m is the real mechanical power which excites the SG. However, the ΔP_{load} is the load of MG which excites the synchronverter. Both of them determine the reference power of the system, and hence, they are the counterparts. Furthermore, based on is inversely proportional to the J, the system inertia)19(frequency droop gain d_{f1}. This relation between inertia and droop gain is also illustrated in [21] for an ac synchronverter.
3) The last term in (17) is not directly modeled in (26). However, this term is virtually equal to the natural dampers of the synchronous generator. According to [20], there are two terms of synchronizing and damping torques in the small signal model of an SG. Each torque which is in the direction of ω-axes (angular velocity of rotor) illustrates the damping torque and each torque which is in the direction of δ-axes (rotor angle) indicates the synchronizing torque. On the other hand, $\omega = d\delta/dt$ and power are related to the angle of rotor. Hence, the derivation of power is in direction of ω-axes and behaves as a damping torque.

Based on the aforementioned analogies between (17) and (26), the dc sources in a dc MG can be controlled like an SG, and hence, they can be coordinated together with an injected frequency without any communication network, and they can operate based on the frequency droop functionality. In the two next sections the viability of the dc synchronverter is evaluated by simulations and experiments.

V. Simulation Results

In order to evaluate the proposed control approach, three case studies are considered for simulations. The simulated system is shown in Fig. 5 and the corresponding parameters are given in Table II. In Case I, power sharing approach between two boost-based Distributed Generators (DGs) with equal ratings is simulated. In Case II, the synchronization of a third converter (e.g., buck-based DG) is demonstrated. Case III shows the performance of the control system in terms of unequal converter ratings as well as motor-based constant power load.

A. Case I: Power sharing between two DGs

In this case, the power sharing between two boost-based DGs are studied. A 3.2 kW load is connected at t = 0.7 *s* and another 2kW load is connected at t = 1.7 *s*. The output current of the converters are shown in Fig. 6, implying a proper load sharing between the two DGs. As it can be seen from Fig. 7, the output voltage of the converters is regulated close to the reference value. Moreover, the injected frequency is shown in Fig. 8, indicating the viability of the proposed frequency-based droop controller, where increasing the load will decrease the injected frequency by the converters. Moreover, the injected frequencies converge to an equal value dictated by the droop gains. For example, as shown in Fig. 6 and Fig. 8, increasing the load by 5 A, causes a frequency drop of 5×0.15 = 0.6 Hz. Therefore, employing the proposed frequency droop controller – inspired from the ac microgrids – improves the power sharing and voltage regulation in dc microgrids.

TABLE II
PARAMETERS OF THE DC MG CONSIDERED FOR SIMULATIONS

Parameter		Symbol	Value		
			Case I	Case II	Case III
Line Impedances		R_1, X_1 R_2, X_2 R_3, X_3	1, 0.06 Ω 1.5, 0.08 Ω 2, 0.1 Ω		
Voltage – power coupling gain		d_p	15 V/VAR		
Frequency droop gain		d_{f1} d_{f2} d_{f3}	0.15 0.15 –	0.15 0.15 0.15	0.15 0.15 0.075
Resistive Loads		P (kW)	3.2, 2	2, 2	2, 2
DC motor	Mechanical speed	ω_m	–	–	150 ras/s
	Mechanical torque	T_m	–	–	25 Nm
	Rotor Inertia	J(Nms^2)	–	–	0.0881
	Armature impedance	R_a, L_a	–	–	0.57 Ω, 4.6 mH
	Field impedance	R_f, L_f	–	–	190 Ω, 0.2 H
	Electrical Power	P (kW)	–	–	3.75
Converters	Inductor	L_{dc}	2 mH		
	Capacitor	C_{dc}	500 μF		

B. Case II: Power sharing and synchronizing considering more than two DGs

In this case, two boost-based DGs are considered with a buck-based DG which is connected to the microgrid at t = 0.1 s. The output current of the converters are shown in Fig. 9, showing the proper synchronization of the third converter. After connecting the third converter, the low frequency oscillations of the third converter is in opposite phase angle of the two other converters. However, the oscillations of the two converters have the similar behavior. This confirms that the MG can be modeled as a single unit when the third converter is connecting.

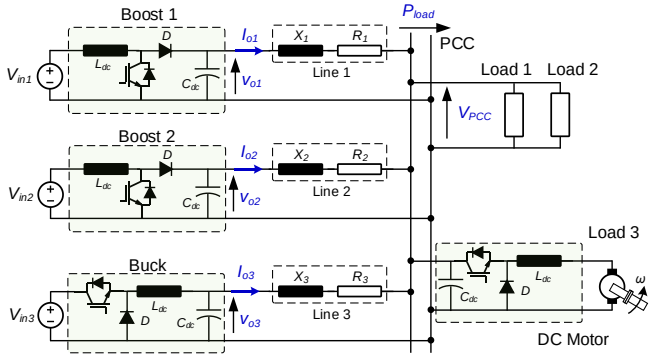

Fig. 5. Block diagram of the simplified dc MG considered for simulations with three power sources, resistive and motor-based constant power load.

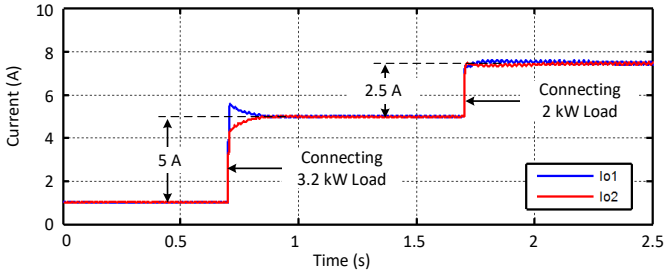

Fig. 6. Simulation results for Case I (see Table II): output current waveforms with the equal converter ratings, V^* = 400 *V*.

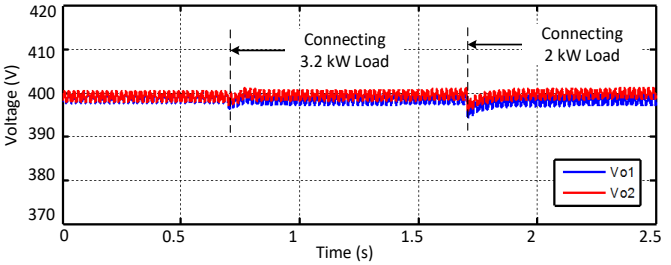

Fig. 7. Simulation results for Case I (see Table II): output voltage waveforms with the equal converter ratings, V^* = 400 *V*.

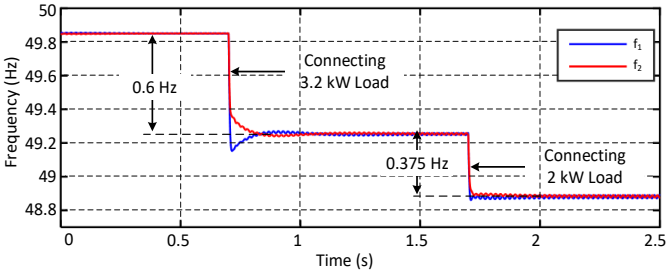

Fig. 8. Simulation results for Case I (see Table II): injected frequencies with the equal converter ratings, V^* = 400 *V*.

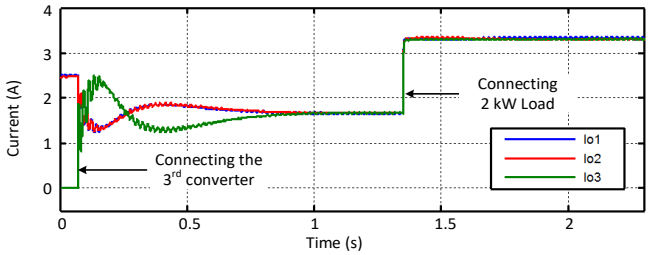

Fig. 9. Simulation results for Case II (see Table II), connecting a 3rd converter: output current waveforms with the equal converter ratings, V^* = 400 *V*.

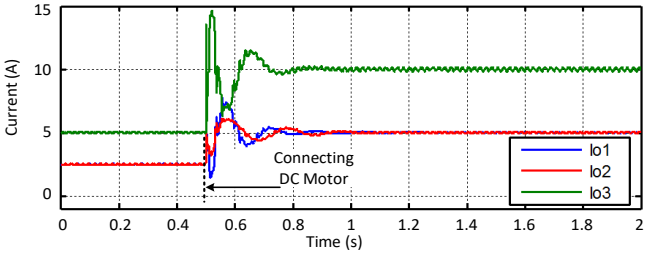

Fig. 10. Simulation results for Case III (see Table II): output current waveforms with the unequal converter ratings, V^* = 400 *V*.

In this case, the equal ratings for the converters are assumed and a proper load sharing is achieved at steady state. Furthermore, after connecting a 2 kW load at t = 1.35 s, the load sharing is also suitably carried out among the converters.

C. Case III: Power sharing among 3 DGs with a constant power load

In order to further evaluate the proposed control system, another case study is considered with a motor-based constant power load. In this case, the power rating of the third converter is two times of the other ones, and hence, it should support the loads two times more than the others. The load and system parameters are given in Table II. At first, the converters are supporting a 4 kW load. At t = 0.5 s, a converter-based motor load – with 25 Nm and 150 rad/s mechanical load – is connected to the microgrid. The output currents of converters are shown in Fig. 10 implying a proper load sharing in the presence of converter-based constant power loads, and the output current of the third converter is 10 *A* and the others are equal to 5 *A*. Furthermore, as shown in Fig. 11, the output voltage of converters is regulated close to the reference value after connecting the motor. The injected frequencies variations are also shown in Fig. 12 and confirming the performance of the frequency droop-based control approach for dc microgrids. As it can be seen in Fig. 12, the injected frequencies by the converters converge to an equal value dictated by the droop characteristics. Simulation results show that controlling the dc converters like an SG results in a suitable load sharing and voltage regulation in dc microgrids.

VI. Experimental Validations

In order to validate the performance of the proposed control approach, a laboratory prototype is implemented following Fig. 13. Two boost converters are connected to loads through line resistances. Each converter is controlled by its own Digital Signal Processor (DSP). The control parameters and system specifications are given in TABLE I. Furthermore, the proportional and integral term of the inner voltage and current controllers are (0.45 + 20/*s*) and (0.05 + 2/*s*) respectively.

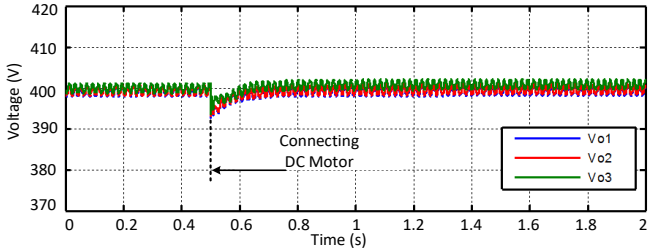

Fig. 11. Simulation results for Case III (see Table II): output voltage waveforms with the unequal converter ratings, V^* = 400 *V*.

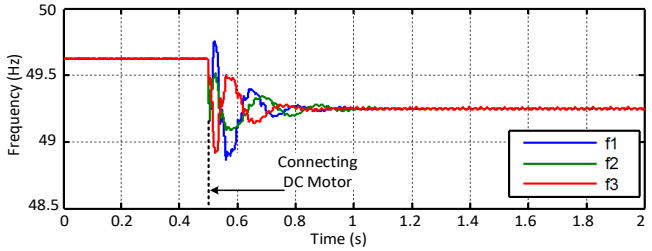

Fig. 12. Simulation results for Case III (see Table II): injected frequencies with the unequal converter ratings, V^* = 400 *V*.

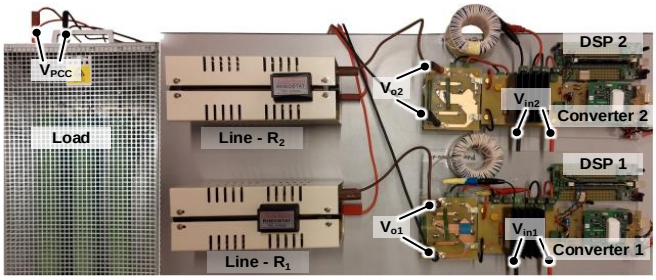

Fig. 13. Photograph of the implemented hardware setup based on two boost converters with R_1 = 2.5 *Ω*, R_2 = 1.5 *Ω*, and P_{load} = 2.5 *kW*.

The test results of the power sharing strategy, synchronization procedure, and efficiency of the proposed approach are addressed in the following. Notably, the performance of the proposed control strategy is experimentally compared with the conventional droop method.

A. Power Sharing Approach

First, the power sharing strategy is verified with equal and unequal converter ratings, and the results are compared with the conventional droop approach. The results of power sharing with equal converter ratings (i.e., d_{f1} = d_{f2} = 0.15) are presented in Fig. 14 showing that the output current of converters are equally shared between converters. The output voltages are also regulated close to 400 *V*. Furthermore, there is a small deviation between dc voltages (ΔV), and ac voltage phases (δ).

The effectiveness of the proposed method is further confirmed by considering different converter capacities ($I_{n,1}$ = 2×$I_{n,2}$) with d_{f1} = 0.5×d_{f2} = 0.15. Since the first and second line resistances are 2.5 and 1.5 *Ω* respectively, a large dc voltage deviation (ΔV) and phase difference (δ) are required in order to perform the proportional current sharing, which is illustrated in Fig. 15. Consequently, the currents are shared proportional to each converter rating, and the dc voltages are settled close to 400 *V*. In order to highlight the performance of the proposed control scheme, an experiment is carried out applying the conventional droop method using the test conditions as in Fig. 15. As it is shown in Fig. 16, applying the conventional droop method, with the droop gain of 5 and 10 *Ω*

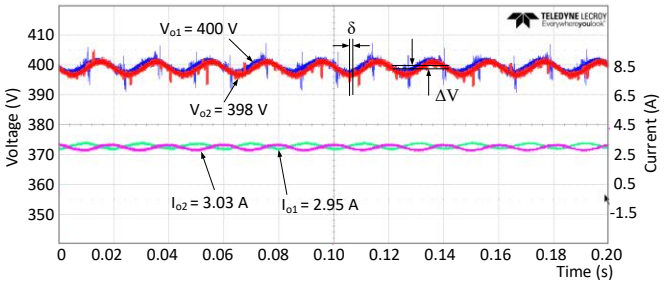

Fig. 14. Experimental results of the proposed method: output voltage and current waveforms with the same converter capacities, $I_{n,1} = I_{n,2}$, $d_{f1} = d_{f2} = 0.15$, $P_{load} = 2.5$ *kW* and $V^* = 400$ *V*.

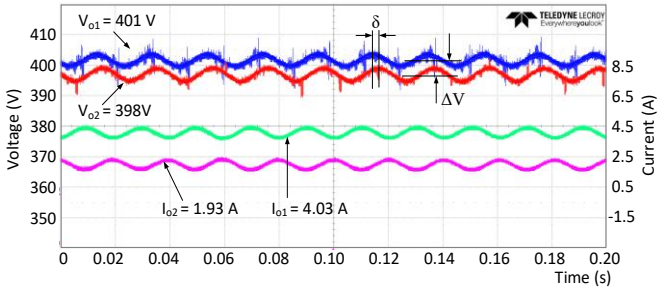

Fig. 15. Experimental results of the proposed method: output voltage and current waveforms with different converter capacities, $I_{n,1} = 2I_{n,2}$, $d_{f1} = 0.5d_{f2} = 0.15$, $P_{load} = 2.5$ *kW* and $V^* = 400$ *V*.

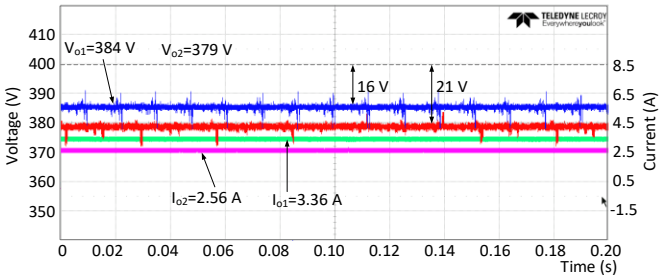

Fig. 16. Experimental results of conventional droop controller: output voltage and current waveforms with different converter capacities, $I_{n,1} = 2I_{n,2}$, $P_{load} = 2.5$ *kW* and $V^* = 400$ *V*.

for the first and second converter, indicates the voltage drop of 16 and 21 *V* from the reference value. Furthermore, the current sharing cannot be proportionally performed between the converters and I_1/I_2 is equal to 1.3 instead of being 2. Therefore, the advantages of the proposed approach in comparison to the conventional droop controller can be summarized as follows:

a) Current sharing performance: employing the proposed control approach causes accurate load sharing between the converters, where the conventional droop method cannot accurately control the load sharing. As shown in Fig. 15, the output current of converters are proportional to the corresponding power ratings, i.e., $I_1/I_2 = I_{n1}/I_{n2} = 2$. However, the conventional droop control results is shown in Fig. 16 implying inaccurate load sharing, i.e., $I_1/I_2 = I_{n1}/I_{n2} = 1.3$.

b) Voltage regulation performance: utilizing the virtual resistances as the conventional droop gains causes large voltage drop in the grid. As shown in Fig. 16, the output voltage of converters are equal to 384 and 379 V. However, following Fig. 15, utilizing the proposed approach the output voltages of converters are regulated close to the nominal voltage value. Therefore, employing the proposed approach brings a suitable voltage regulation in the grid.

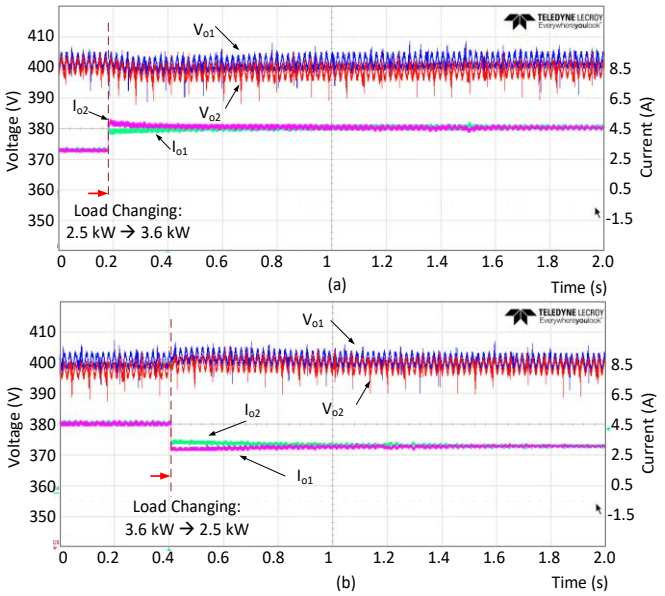

Fig. 17. Experimental results with equal converter ratings: dynamic response of the proposed control system under load variation from (a) 2.5 kW to 3.6 kW and (b) 3.6 kW to 2.5 kW – $I_{n,1} = I_{n,2}$, $d_{f1} = d_{f2} = 0.15$, and $V^* = 400$ *V*.

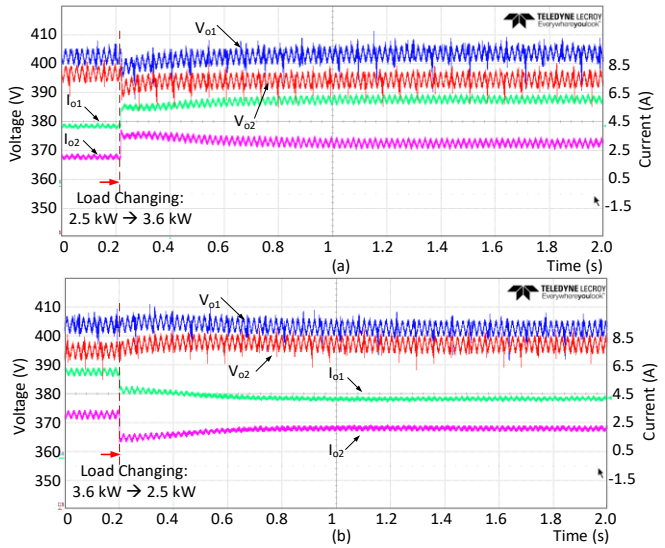

Fig. 18. Experimental results with unequal converter ratings: dynamic response of the proposed control system under load variation from (a) 2.5 kW to 3.6 kW and (b) 3.6 kW to 2.5 kW – $I_{n,1} = 2I_{n,2}$, $d_{f1} = 0.5d_{f2} = 0.15$, and $V^* = 400$ *V*.

Fig. 17 shows the experimental load transient performance of the proposed control approach for equal converter ratings under load variations from 2.5 *kW* to 3.6 *kW* and from 3.6 *kW* to 2.5 *kW* respectively. As it can be seen, in both cases, the load is equally shared between the converters and the output voltage of converters is regulated close to 400 *V*. Furthermore, as it is illustrated in Fig. 18, the dynamic response of system with unequal converter ratings is also evaluated for a sudden 1.1 *kW*-load increase and decrease respectively. In both cases, voltage regulation and load sharing are properly carried out with fast response time and without major voltage drop.

B. Synchronization Verification (with PLL & without PLL)

The synchronization procedure with utilizing a PLL is shown in Fig. 19, where the first converter is initially turned on, and at t_1, the second converter is connected. After 0.1 *s*,

the PLL of the second converter extracts the phase of ac voltage and the second converter at t_2, injects the ac voltage. Therefore, both converters are properly synchronized and the currents are shared among the converters.

However, as already mentioned, the converters can be synchronized without using a PLL since the amplitude of the injected voltage and consequently the ac current are very small and the ac signals can be synchronized based on the droop controller functionality. The synchronization result without a PLL is shown in Fig. 20, where the first converter is connected at t = 0.2 s. As it can be seen, both converters are properly synchronized.

C. Efficiency Evaluation

Furthermore, in order to investigate the effect of the proposed approach on the power converter efficiency, as depicted in Fig. 20 experimental measurements are performed. The obtained results show that applying the proposed scheme does not significantly impact the power converter efficiency comparing with the conventional droop method. This is due to the relatively small amplitude of the injected ac voltages and currents. For instance, the measured overall system efficiency for the two experiments illustrated in Fig. 15 (proposed method) and Fig. 16 (conventional method) is 94.8% and 95.9%, respectively.

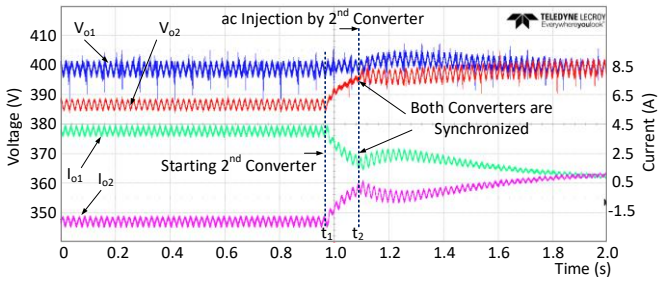

Fig. 19. Experimental results of synchronization procedure with a PLL. First converter is turned on and second converter is connected at t_1, after 0.1 s, at t_2, the second converter injects ac voltage and both converters are synchronized.

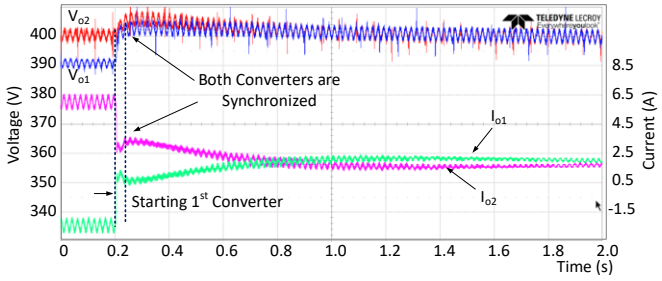

Fig. 20. Experimental results of synchronization procedure without PLL. First converter is connected at 0.2 *s*, and both converters are synchronized.

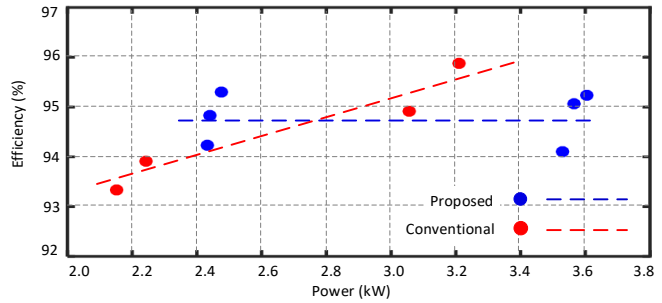

Fig. 21. Experimental results, overall efficiency of the proposed method and conventional method, dashed lines are obtained by curve fitting.

In order to find out the differences between the two efficiency curve, it is fruitful to mention that in the conventional approach, the dc link voltage is decreased by increasing the load power due to the droop gains, and hence the switching and conduction losses of the system are decreased. Therefore, the efficiency of the system will be increased by increasing the load power. However, in the proposed method, the dc link voltage is regulated close to the reference value. Therefore, the efficiency of the proposed approach should not be increased by increasing the load power unlike the conventional method.

VII. Conclusion

This paper has presented a power sharing approach based on the concept of synchronverter for LVDC microgrids. DC sources are coordinated together with an injected frequency, and hence, the power sharing is properly performed utilizing frequency droop controller. Moreover, the dc voltage drops due to the conventional droop controller do not exist in the proposed approach, and hence an acceptable voltage regulation can be obtained. The small signal stability of the proposed method and mathematical analysis to illustrate the analogy between dc synchronverter and SG are explained. The effectiveness of the proposed control system is evaluated by simulations including two and three converters as well as resistive and motor-based constant power loads. Finally, load sharing and voltage regulation performance of the proposed method with equal and unequal converter ratings as well as dynamic response of the control system and synchronization procedure are experimentally verified. Furthermore, the performance of the proposed approach in comparison to the conventional droop controller is verified by experiments implying an accurate current sharing and acceptable voltage regulation with the proposed approach. Moreover, the efficiency of the proposed method is experimentally compared to the conventional droop controller and the results show that an acceptable efficiency is achieved by employing the proposed strategy compared to the conventional approach.

References

[1] B. T. Patterson, "DC, Come Home: DC Microgrids and the Birth of the 'Enernet,'" *IEEE Power Energy Mag.*, vol. 10, no. 6, pp. 60–69, 2012.

[2] A. Sannino, G. Postiglione, and M. H. J. Bollen, "Feasibility of a DC Network for Commercial Facilities," *IEEE Trans. Ind. Appl.*, vol. 39, no. 5, pp. 1499–1507, 2003.

[3] M. E. Baran and N. R. Mahajan, "DC Distribution for Industrial Systems: Opportunities and Challenges," *IEEE Trans. Ind. Appl.*, vol. 39, no. 6, pp. 1596–1601, 2003.

[4] T. Dragicevic, J. M. Guerrero, J. C. Vasquez, and D. Skrlec, "Supervisory Control of an Adaptive-Droop Regulated DC Microgrid with Battery Management Capability," *IEEE Trans. Power Electron.*, vol. 29, no. 2, pp. 695–706, 2014.

[5] Y. Gu, X. Xiang, W. Li, and X. He, "Mode-Adaptive Decentralized Control for Renewable DC Microgrid With Enhanced Reliability and Flexibility," *IEEE Trans. Power Electron.*, vol. 29, no. 9, pp. 5072–5080, 2014.

[6] S. Moayedi and A. Davoudi, "Distributed Tertiary Control of DC Microgrid Clusters," *IEEE Trans. Power Electron.*, vol. 31, no. 2, pp. 1717–1733, 2015.

[7] S. Anand, B. G. Fernandes, and J. M. Guerrero, "Distributed Control to Ensure Proportional Load Sharing and Improve Voltage Regulation in Low-Voltage DC Microgrids," *IEEE Trans. Power Electron.*, vol. 28, no. 4, pp. 1900–1913, 2013.

[8] A. Khorsandi, M. Ashourloo, and H. Mokhtari, "A Decentralized Control Method for a Low-Voltage DC Microgrid," *IEEE Trans. Energy*

Convers., vol. 29, no. 4, pp. 793–801, 2014.
[9] X. Lu, J. M. Guerrero, K. Sun, and J. C. Vasquez, "An Improved Droop Control Method for DC Microgrids Based on Low Bandwidth Communication With DC Bus Voltage Restoration and Enhanced Current Sharing Accuracy," *IEEE Trans. Power Electron.*, vol. 29, no. 4, pp. 1800–1812, Apr. 2014.
[10] J. M. Guerrero, J. C. Vasquez, J. Matas, L. G. De Vicuña, and M. Castilla, "Hierarchical Control of Droop-Controlled AC and DC Microgrids - A General Approach toward Standardization," *IEEE Trans. Ind. Electron.*, vol. 58, no. 1, pp. 158–172, 2011.
[11] V. Nasirian, A. Davoudi, and F. L. Lewis, "Distributed Adaptive Droop Control for Dc Microgrids," *IEEE Trans. Energy Convers.*, vol. 29, no. 4, pp. 1147–1152, 2014.
[12] P.-H. Huang, P.-C. Liu, W. Xiao, and M. S. El Moursi, "A Novel Droop-Based Average Voltage Sharing Control Strategy for DC Microgrids," *IEEE Trans. Smart Grid*, vol. 6, no. 3, pp. 1096–1106, May 2015.
[13] S. Peyghami-Akhuleh, H. Mokhtari, P. C. Loh, and F. Blaabjerg, "Distributed Secondary Control in DC Microgrids with Low-Bandwidth Communication Link," in *Proc. IEEE PEDSTC*, 2016, pp. 641–645.
[14] S. Peyghami-Akhuleh, H. Mokhtari, P. Davari, P. Chang Loh, and F. Blaabjerg, "Smart Power Management of DC Microgrids in Future Milligrids," in *Proc. IEEE EPE ECCE Europe*, 2016.
[15] A. Khorsandi, M. Ashourloo, H. Mokhtari, and R. Iravani, "Automatic Droop Control for a Low Voltage DC Microgrid," *IET Gener. Transm. Distrib.*, vol. 10, no. 1, pp. 41–47, Jan. 2016.
[16] D. Perreault, R. Selders, and J. Kassakian, "Frequency-Based Current-Sharing Techniques for Paralleled Power Converters," *IEEE Trans. Power Electron.*, vol. 13, no. 4, pp. 626–634, 1998.
[17] A. Tuladhar, H. Jin, T. Unger, and K. Mauch, "Control of Parallel Inverters in Distributed AC Power Systems with Consideration of Line Impedance Effect," *IEEE Trans. Ind. Appl.*, vol. 36, no. 1, pp. 131–138, 2000.
[18] A. Tuladhar, H. Jin, T. Unger, and K. Mauch, "Parallel Operation of Single Phase Inverter Modules with No Control Interconnections," in *Proc. IEEE APEC*, 1997, vol. 1, pp. 94–100.
[19] A. Tuladhar and H. Jin, "A Novel Control Technique to Operate DC/DC Converters in Parallel with No Control Interconnections," in *Proc. IEEE PESC*, 1998, vol. 1, pp. 892–898.
[20] P. Kundur, N. Balu, and M. Lauby, "*Power System Stability and Control*." New York: McGraw-hill, 1994.
[21] M. Karimi-Ghartemani, "Universal Integrated Synchronization and Control for Single-Phase DC/AC Converters," *IEEE Trans. Power Electron.*, vol. 30, no. 3, pp. 1544–1557, 2015.
[22] Q. Zhong and G. Weiss, "Synchronverters: Inverters That Mimic Synchronous Generators," *IEEE Trans. Ind. Electron.*, vol. 58, no. 4, pp. 1258–1267, 2011.
[23] P. Frack, P. Mercado, M. Molina, E. Watanabe, R. De Doncker, and H. Stagge, "Control-Strategy for Frequency Control in Autonomous Microgrids," *IEEE J. Emerg. Sel. Top. Power Electron.*, vol. 3, no. 4, pp. 1046–1055, 2015.
[24] Q. Shafiee, T. Dragicevic, J. C. Vasquez, and J. M. Guerrero, "Hierarchical Control for Multiple DC-Microgrids Clusters," *IEEE Trans. Energy Convers.*, vol. 29, no. 4, pp. 922–933, 2014.
[25] Q. Shafiee, J. M. Guerrero, and J. C. Vasquez, "Distributed Secondary Control for Islanded Microgrids—A Novel Approach," *IEEE Trans. Power Electron.*, vol. 29, no. 2, pp. 1018–1031, 2014.
[26] J. M. Guerrero, L. Hang, and J. Uceda, "Control of Distributed Uninterruptible Power Supply Systems," *IEEE Trans. Ind. Electron.*, vol. 55, no. 8, pp. 2845–2859, 2008.
[27] J. Rocabert, A. Luna, F. Blaabjerg, and P. Rodriguez, "Control of Power Converters in AC Microgrids," *IEEE Trans. Power Electron.*, vol. 27, no. 11, pp. 4734–4749, 2012.

Saeed Peyghami (S'14) was born in Tabriz, Iran, in 1988. He received the B.Sc. and M.Sc. degrees both in electrical engineering from the Department of Electrical Engineering, Sharif University of Technology, Tehran, in 2010 and 2012, respectively. He is currently working toward the Ph.D. degree in electrical engineering at Sharif University of Technology, Tehran, Iran.

His research interests include power electronics system control, power quality, application of power electronics in distributed power systems.

Pooya Davari (S'11–M'13) received the B.Sc. and M.Sc. degrees in electronic engineering from University of Mazandaran (Noushirvani), Babol, Iran, in 2004 and 2008, respectively, and the Ph.D. degree in power electronics from Queensland University of Technology (QUT), Brisbane, Australia, in 2013. From 2005 to 2010, he was involved in several electronics and power electronics projects as a Development Engineer. During 2010–2014, he investigated and developed high-power, high-voltage power electronic systems for multidisciplinary projects such as ultrasound application, exhaust gas emission reduction, and tissue-materials sterilization. From 2013 to 2014 he was with QUT, as a Lecturer. He joined the Department of Energy Technology, Aalborg University, Aalborg, Denmark, as a Postdoctoral Researcher in August 2014, where he is currently an Assistant Professor. His current research interests include active front-end rectifiers, harmonic mitigation in adjustable-speed drives, electromagnetic interference (EMI) in power electronics, high power density power electronic systems, and pulsed power applications. Dr. Davari was awarded a research grant from the Danish Council of Independent Research (DFF-FTP) in 2015 and he is currently serving as an editor of the International Journal of Power Electronics.

Hossein Mokhtari (M'03–SM'14) was born in Tehran, Iran, on August 19, 1966. He received the B.Sc. degree in electrical engineering from Tehran University, Tehran, in 1989. He received the M.Sc. degree in power electronics from the University of New Brunswick, Fredericton, NB, Canada, in 1994, and the Ph.D. degree in power electronics/power quality from the University of Toronto, Toronto, ON, Canada in 1999.

From 1989 to 1992, he worked in the Consulting Division of Power Systems Dispatching Projects, Electric Power Research Center Institute, Tehran. Since 2000, he has been with the Department of Electrical Engineering, Sharif University of Technology, Tehran, where he is currently a Professor. He is also a Senior Consultant to several utilities and industries.

Poh Chiang Loh received his B.Eng (Hons) and M.Eng degrees from the National University of Singapore, Singapore, Singapore, in 1998 and 2000, respectively, and the Ph.D degree from Monash University, Melbourne, Vic., Australia, in 2002, all in electrical engineering.

His interests are in power converters and their grid applications.

Frede Blaabjerg (S'86–M'88–SM'97–F'03) was with ABB-Scandia, Randers, Denmark, from 1987 to 1988. From 1988 to 1992, he was a Ph.D. Student with Aalborg University, Aalborg, Denmark. He became an Assistant Professor in 1992, Associate Professor in 1996, and Full Professor of power electronics and drives in 1998. His current research interests include power electronics and its applications such as in wind turbines, PV systems, reliability, harmonics and adjustable speed drives.

He has received 17 IEEE Prize Paper Awards, the IEEE PELS Distinguished Service Award in 2009, the EPE-PEMC Council Award in 2010, the IEEE William E. Newell Power Electronics Award 2014 and the Villum Kann Rasmussen Research Award 2014. He was an Editor-in-Chief of the IEEE TRANSACTIONS ON POWER ELECTRONICS from 2006 to 2012. He is nominated in 2014 and 2015 by Thomson Reuters to be between the most 250 cited researchers in Engineering in the world.